2013 IEEE/RSJ International Conference on
Intelligent Robots and Systems (IROS)
November 3-7, 2013. Tokyo, Japan

Calibrating Setups with a Single-Point Laser Range Finder and a Camera

Thanh Nguyen[1] and Gerhard Reitmayr[2]

Abstract— **The combination of a cheap single-point laser range finder (LRF) device and cameras has become increasingly useful in recent research and industrial applications. While the single dot laser range finder can only provide depth for a single pixel in the observed image, it's cost and size can be useful for handheld devices or very lightweight robotic platforms. In this work, we propose two accurate calibration methods for determining the position and direction of the laser range finder with respect to the camera. Notably, we can determine the full calibration, even without observing the laser range finder observation point in the camera image. We evaluate both methods on synthetic and real data demonstrating their efficiency and good behavior under noise.**

I. Introduction

The combination of a cheap single-point laser range finder (LRF) device and cameras has become increasingly useful in recent research and industrial applications [1], [2]. While the single dot laser range finder can only provide depth for a single pixel in the observed image, it's cost and size can be useful for handheld devices or very lightweight robotic platforms. The calibration of such setups is therefore of considerable interest. In this work, we propose two accurate calibration methods for determining the position and direction of the laser range finder with respect to the camera. The first method observes the laser dot on the known target plane to add constraints on the 3D location of the measured point. Fig. 1a illustrates the detailed setup for this method. The second method only uses the distance measurement from the laser range finder as constraint, thereby avoiding the requirement to observe the laser dot location in the image. Fig. 1b visualizes this second measurement setup. Both methods integrate with standard camera calibration methods [3], and offer a very simple calibration procedure. From our best knowledge, our methods are the first in literature to tackle calibration issue for this setup.

2D, scanning or 3D laser range finders, which distance to many points simultaneously, are well-known in literature [4], and have been widely used, especially in robotics [5], [6], [7], [8], [13]. However, such *multi-points* LRFs are usually expensive and heavy, limiting the use in small and lightweight devices. Therefore some researchers looked to more affordable single-point LRFs, for example, Patel et. al. [1] and Wither et. al. [2] proposed to use such single-point LRFs in their augmented reality systems. In recent years, single-point LRFs were further miniaturized and can be found in inexpensive measurement tools. Nowadays, mobile devices can be easily equipped with a single-point LRF model [2], [10]. These devices open new opportunities for a wide range of applications which have been impractical previously. Therefore, a simple and accurate calibration procedure for systems comprising a single-point LRF and a camera is required.

Several calibration methods have been proposed for the setup of *multi-points* LRF and camera in literature. One widely known calibration method by Zhang and Pless [3] calibrates the camera intrinsic parameters and *multiple-points*, on projective line, LRF's relative pose with respect to the camera. Besides, Unnikrishnan and Hebert [11] developed a fast and easy to use software which allows to calibrate camera intrinsics and relative pose of 3D LRF. Recently, Vasconcelos et. al. [4] introduced new calibration method which requires a minimal of three captured plane poses for the setup of *multiple-points*, on projective line, LRF and camera such as in Zhang and Pless's setup; however, Vasconcelos et. al. focused only on calibrating the relative pose between LRF and camera while assuming that the camera's intrinsics are well calibrated beforehand.

Although calibration for the setup of single-point LRF and camera can benefit from the methods discussed, espeically the method proposed by Zhang and Pless [3]. However, our calibration of the relative pose between single-point LRF and camera requires a different approach, where laser range observation is limited to single point per video frame. This poses different challenges regarding prior work. Additionally, global optimization to refine camera's intrinsics and the relative pose must be constructed with different formulas.

In this work, we propose two methods to tackle the challenges of extrinsic single-point LRF and camera calibration. Our evaluation results show that the proposed methods are highly accurate and efficient. Furthermore, we offer an easy to use software implementation demonstrating a complete, simple calibration procedure.

II. Method

A. Common preliminaries

Our calibration methods integrate with the standard camera calibration methods that use the observations of a known planar target pattern from different camera poses. We assume that n images $I_i, i = 1 \ldots n$ of the target were recorded and that through camera calibration, both the intrinsic parameters of the camera and the n extrinsic pose parameters p_i for each image I_i were estimated. Thus, the pose of planar target is

[1]Thanh Nguyen is with Department of Computer Science, Graz University of Technology, 8010 Graz, Austria thanh@icg.tugraz.at

[2]Gerhard Reitmayr is with the Department of Computer Scienece, Graz University of Technology, 8010 Graz, Austria reitmayr@icg.tugraz.at

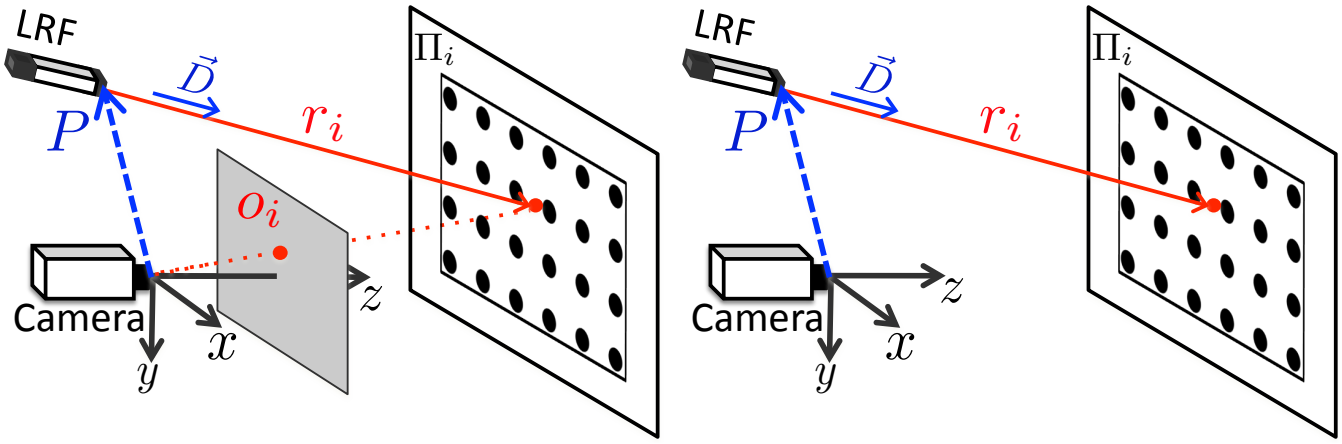

(a) (b)

Fig. 1: Method 1 (left) uses the pose of a calibration target plane Π_i, the distance of a point on the plane r_i and the observation of the laser dot on the same point in the camera image O_i. Method 2 (right) dispenses with the observation of the laser dot and only uses the plane pose and distance measurement.

known for each image. The pose is fully determined and in real world units, because the target pattern dimensions are known in real world units.

Camera intrinsics and extrinsics calibration: Camera calibration aims to find intrinsic parameters and extrinsic parameters of the camera.

Given world 3D point $[X_w, Y_w, Z_w]^T$, and transformation $pose = [R|t]$, 3D point in camera coordinates is:

$$\begin{bmatrix} x_c & y_c & z_c \end{bmatrix}^T = R \begin{bmatrix} X_w & Y_w & Z_w \end{bmatrix}^T + t^T \quad (1)$$

$$x' = x_c/z_c, y' = y_c/z_c, r = \sqrt{(x'-c_x)^2 + (y'-c_y)^2} \quad (2)$$

Camera's lens distortion model is formulated as radial distortion, thus we have

$$x'' = x'(1 + k_1 r^2 + k_2 r^4) \qquad y'' = y'(1 + k_1 r^2 + k_2 r^4)$$

where k_1, k_2 are radial distortion coefficients.

Camera linear model is formed as a 2x3 matrix (4DOF):

$$\begin{pmatrix} u \\ v \end{pmatrix} = \begin{bmatrix} f_x & 0 & c_x \\ 0 & f_y & c_y \end{bmatrix} * \begin{pmatrix} x'' \\ y'' \end{pmatrix} \quad (3)$$

where f_x, f_y are focals, c_x, c_y are principle point coordinates on image plane, and u, v are in pixel coordinates.

The camera calibration is formulated as non-linear optimization of the following objective equation:

$$O_{cam} = \sum_{i,j} \left\| \begin{bmatrix} u_j \\ v_j \end{bmatrix} - camproj(pose_i * W_j) \right\|_2 \quad (4)$$

where $W_j = [X_j, Y_j, Z_j]^T$ are known 3D points of the calibration target, $[u_j, v_j]^T$ is the 2D pixel location observations of the 3D points, and $camproj()$ function is to map 3D point in camera coordinate to image plane. For $camproj()$, it is described in Eq. (1), (2) and (3).

Algorithm 1 Calibrate camera intrinsics and LRF extrinsics.

Require: Known planar target with 3D point positions.
Ensure: Camera parameters $(f_x, f_y, c_x, c_y, k_1, k_2)$,
Laser range finder position P and direction D.

1: Estimate plane poses Π_i and camera intrinsics $(f_x, f_y, c_x, c_y, k_1, k_2)$ using camera calibration.
2: Setup linear constraints for LRF parameters for each Π_i, using Eq. (7) for Method 1 or Eq. (9) for Method 2.
3: Solve LRF parameters $(P, D)^T$ from linear constraints.
4: Refine estimated LRF parameters using Eq. (10).
5: Refine camera intrinsics and LRF parameters $(P, D)^T$ jointly in Eq. (10).

B. The Algorithm

Algorithm 1 provides an overview of the proposed estimation method for complete camera and single-point LRF calibration. In step (1) applies well-known camera calibration techniques [3] to calibrate the camera intrinsics and pose of the calibration target. Given camera intrinsics and plane poses, we obtain a system of linear equations for the LRF extrinsics (step (2)) and solve it (step (3)). The linear equations in step (3) guatantee a closed form solution which is relatively close to the optimal solution. Therefore, nonlinear least square optimization of the objective function in Eq. 10 can be applied in order to refine the initial estimated LRF extrinsics. Finally, global bundle adjustment is applied to solve the same objective function as before; however, we now adjust camera intrinsics, plane poses, and LRF extrinsics simultaneously. The final step is only necessary when there are much noise in measurements.

C. Method 1: Laser Dot and Range Observations

The first method effectively measures a set of 3D points both in the LRF coordinate system as well as in the camera coordinate system (see Fig. 2). Then a 5 DoF transformation

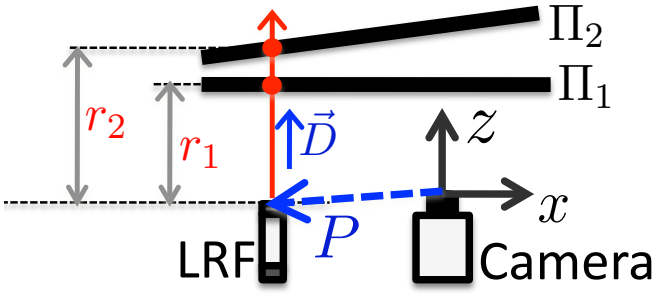

Fig. 2: Top-down view of 3D geometry of Method 1.

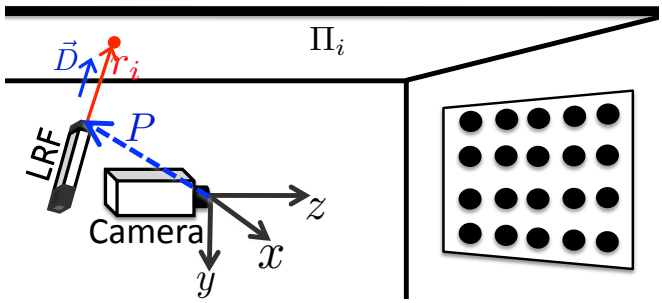

Fig. 3: One sample setup where the laser dot is oblique.

between the two coordinate systems can be estimated, while the rotation around the axis of the laser is undefined. We represent the transformation as the point of origin of the laser P and the direction D in the camera coordinate system. The direction is assumed to be of unit length $\|D\| = 1$ which provides the 2D rotation freedoms.

A 3D point X measured by the laser range finder can be represented in camera coordinates using the origin of the laser P and direction D as

$$X = \begin{pmatrix} P_x + r \cdot D_x \\ P_y + r \cdot D_y \\ P_z + r \cdot D_z \end{pmatrix} = P + r \cdot D. \tag{5}$$

The same point X can be observed in the camera image, if it lies on the calibration target plane and the laser creates a dot that can be detected. Then the point's 3D coordinates are given by re-projecting the image observation $(u,v)^T$ back onto the plane $\Pi = \begin{pmatrix} a & b & c & d \end{pmatrix}$

$$X = \frac{-d}{au + bv + c} \begin{pmatrix} u \\ v \\ 1 \end{pmatrix} = z \begin{pmatrix} u \\ v \\ 1 \end{pmatrix}. \tag{6}$$

Setting equation (5) equal to (6) and rewriting for the unknowns $(P,D)^T$ provides 3 linear constraints from a single image

$$\begin{pmatrix} \mathbb{I} & r \cdot \mathbb{I} \end{pmatrix} \begin{pmatrix} P \\ D \end{pmatrix} = z \begin{pmatrix} u \\ v \\ 1 \end{pmatrix}. \tag{7}$$

Given two or more images observing the calibration target and the laser dot on the target plane, the equations in (7) are stacked for the observations and solved for the vector of unknowns $(P,D)^T$ in a least squares sense.

Existence of a solution: The system is solvable as long as two different points on the laser ray are measured, and therefore two different distances r_i are observed. Then the system is of rank 6 and solvable.

D. Method 2: Range Observations Only

Image processing for detecting the laser dot may not always be feasible, depending on lighting situation, calibration target and the LRF device itself. Furthermore, some applications require the LRF to measure points outside the camera's field of view. For example the Hedgehog tracking system [12] uses a set of lasers to cover different directions. Fig. 3 shows a model of such a setup.

To address these situations, we propose a second method which uses only range observations while requiring that the laser beam hits a reference plane that is known relative to the camera. Without loss of generality, we assume that the laser beam hits the calibration target plane, but any other plane rigidly connected to it is also viable. It is shown from the work of Wei and Hirzinger [13] that calibration for these situations can be solved without requiring knowledge about a reference plane. In contrast, our method specializes on setups which the reference plane is known. Consequently, we can achieve more efficient calibration method.

Given again the target plane $\Pi = \begin{pmatrix} a & b & c & d \end{pmatrix}$, we now only assume that the LRF measures the distance to a point on that plane. Therefore the 3D point X given by (5) must coincide with the plane Π. This leads to the following linear equation

$$\Pi \cdot X = \begin{pmatrix} a & b & c & d \end{pmatrix} \cdot \begin{pmatrix} P_x + r \cdot D_x \\ P_y + r \cdot D_y \\ P_z + r \cdot D_z \\ 1 \end{pmatrix} = 0. \tag{8}$$

Eq. (8) can be rearranged in the unknowns $(P,D)^T$ to obtain a single linear constraint

$$\begin{pmatrix} \begin{pmatrix} a & b & c \end{pmatrix} & r \cdot \begin{pmatrix} a & b & c \end{pmatrix} \end{pmatrix} \begin{pmatrix} P \\ D \end{pmatrix} = -d. \tag{9}$$

Using at least 6 input images, we obtain 6 or more constraints and can solve the resulting system for the unknowns $(P,D)^T$. Again similar to II-C, we also obtain any scale difference between the camera coordinate system and the LRF coordinate system.

Existence of a solution: To obtain a solution, the matrix of constraints must have full rank 6. For the first 3 columns, full rank implies that the normal vectors of all planes span a space of rank 3. This implies that the planes cannot all be parallel, or be parallel to a single direction in space. Furthermore, the second 3 columns are the same set of normal vectors, but scaled by different ranges. Again, to add further 3 ranks, the ranges should differ between the individual planes. Overall, if the camera/LRF setup is moved to different distances from the target plane and into orientations covering all 3 space, then the matrix will be of full rank.

E. Bundle Adjustment

Zhang and Pless [3] demonstrated that applying refinement to camera intrinsics, plane poses, and LRF relative pose in a global bundle adjustment enhances overall accuracy. In this work, we used a similar approach to do non-linear refinement on the camera intrinsics, plane poses, and LRF relative pose. We minimize a single energy function comprising two terms: reprojection error and LRF distance error as given by equations (7) and (9). The first term is to adjust camera intrinsics and plane poses, while the second term refines the LRF relative pose.

$$O = \sum_{i,j} \left\| \begin{pmatrix} u_j \\ v_j \end{pmatrix} - camproj(pose_i * W_j) \right\|^2 + E \qquad (10)$$

For method 1, the objective function E in equation (10) is as follows

$$E = \sum_i \left\| \begin{pmatrix} \mathbb{I} & r_i \cdot \mathbb{I} \end{pmatrix} \begin{pmatrix} P \\ D \end{pmatrix} - z_i \begin{pmatrix} u_i \\ v_i \\ 1 \end{pmatrix} \right\|^2 + (\|D\|^2 - 1)^2 \qquad (11)$$

And, for method 2, the objective function E in equation (10) is

$$E = \sum_i \left\| \begin{pmatrix} \Pi_i & r_i \cdot \Pi_i \end{pmatrix} \begin{pmatrix} P \\ D \end{pmatrix} + d_i \right\|^2 + (\|D\|^2 - 1)^2 \qquad (12)$$

In equation (11) and (12), we used the second term to normalize the length of the laser direction D.

III. Evaluation

In this section, we evaluate the two methods on synthetic and real data, focusing on the estimated laser position and direction. The experiments with synthetic data evaluate the performance under the influence of noise, and the number of measurements used. The real data validates the accuracy results from the simulation.

A. Synthetic Data

In order to generate perfect ground truth data, we simulate the imaging and distance measurement process. We use the camera intrinsics of a real camera at image resolution 640x480, and simulate 100 plane poses at different distances and orientation. Furthermore, we define the LRF parameters $(P,D)^T$. Then, for each plane pose, we calculate the re-projection of a grid of 3D points on the plane, and simulate a laser distance measurement by intersecting the plane with the laser line. The re-projection of the intersection point provides the 2D observation of the laser dot, while the distance to the laser position is the range measurement.

Firstly, we investigate the performance of the two proposed calibration methods under different noise magnitudes. We simulate camera observation noise by adding 2D Gaussian noise ($\sigma = 1$ pixel) to the pixel observations, and laser range noise by adding Gaussian noise ($\sigma = 2mm$) to the distance measurements. For different noise levels, we scale the default standard deviations by a factor in the range $[0.25 - 3.0]$. For this investigation, we use 3 poses for Method 1 and 7 poses for Method 2. For each method, we run 100 trials with different subsets of poses from the simulated set.

We evaluate three different conditions: (I) camera noises only, (II) laser range noise only and (III) both sources of noise. Fig. 4 illustrates the errors in estimating LRF position and direction for the two methods. The position error is the distance between estimated and ground truth position, while the direction error is the angle between estimated and ground truth direction.

The errors grow respectively with noise magnitude as expected. Furthermore, Method 1 has smaller errors in all the cases comparing to Method 2, because it uses more information from each image. For Method 1, the direction error is independent from the laser noise, as the laser measurement only defines the laser position P on the line in space (see Fig. 2).

A second evaluation looks at the influence of the number of measurements on accuracy. We use between 2 to 20 poses for Method 1, and 6 to 20 poses for Method 2 and generated for each number of poses 100 random trials. In all cases a fixed Gaussian noise with $\sigma = 1$pixels on camera measurements and $\sigma = 2mm$ on laser measurements was used. Fig. 5 shows estimation errors as functions of the number of measurements used. Both methods improve significantly with more than the minimal set of measurements. With 10 measurements or more, Method 1 reaches an acceptable level (below $10^{-2}m$ position error and around 10^{-1} angular error). Method 2 needs 20 measurements or more to reach a comparable accuracy.

We also observed that Method 2 is more sensitive to the distribution of angles under which the calibration target is seen. This is directly related to the linear system which is better conditioned of the normal vectors of the plane cover a larger part of the space.

B. Empirical Experiments

For evaluation on real data, we captured 100 plane poses at random positions. Similar to the synthetic data, we evaluate the two methods on different numbers of plane poses: 2 to 20 poses for Method 1, and 6 to 20 poses for Method 2. We run 100 trials for each number of plane poses, randomly chosen from the recorded 100 poses. Since no ground truth data is available, we plot the distribution of the estimated parameters (see Fig. 6) to demonstrate the reliability of the proposed methods.

The empirical evaluation results largely confirm our evaluation on synthetic data for both Method 1 and Method 2. Moreover, it shows that in an empirical setup, Method 2 performs comparative to Method 1 when the number of plane poses is from 8 to 12; and Method 2 slightly outperforms Method 1 with larger number of poses. This seems contradict to our synthetic evaluation whereas Method 1 has mostly smaller errors comparing to Method 2. This indicates that a major source of error in Method 1 is the accuracy of the laser dot detection in the corresponding video image. This source of error in reality is much larger than our noise simulation in the synthetic evaluation. In our experiments, the accuracy

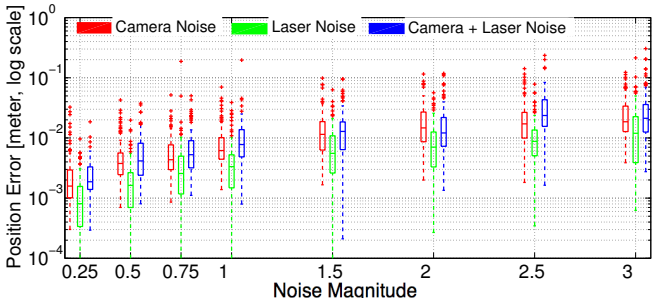

(a) Method 1: Position Error

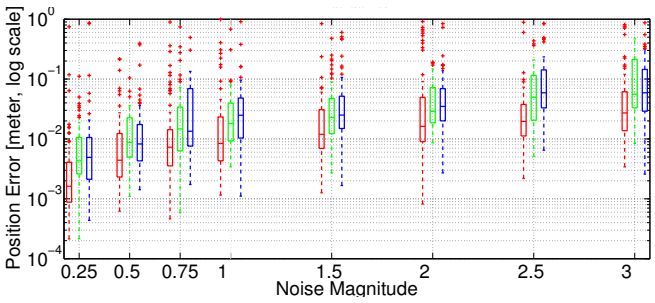

(b) Method 2: Position Error

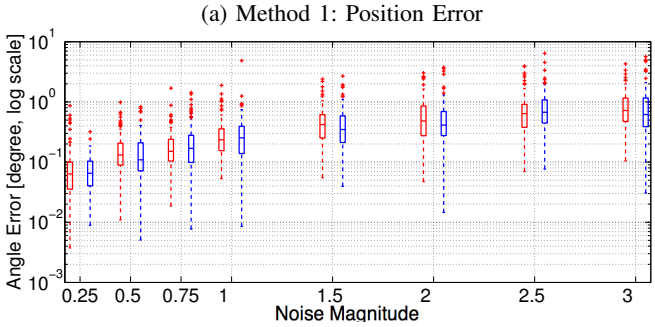

(c) Method 1: Direction Angle Error

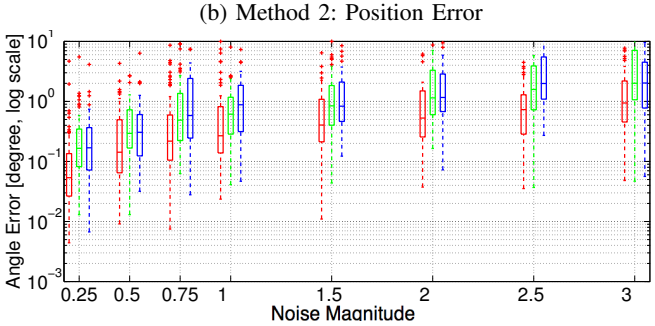

(d) Method 2: Direction Angle Error

Fig. 4: Error distribution under noise levels in the range of $[0.25-3.0]$ simulated on synthetic data for Method 1 (left column) and Method 2 (right column). The boxes illustrate the position error (first row) and angular error of the direction (second row) where the box shows the $25\%-75\%$ quantiles, and the whiskers to 99.3%. In (c) the laser noise does not influence the direction, therefore there is no direction error in this case.

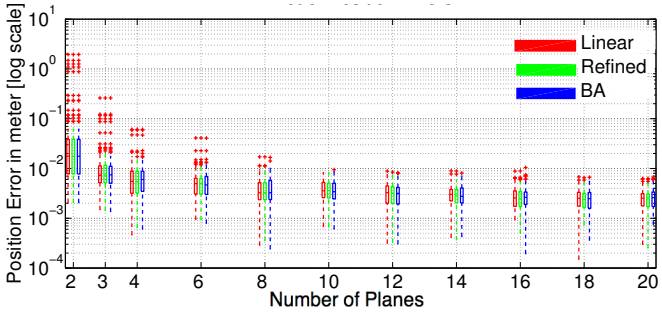

(a) Method 1: Position Error

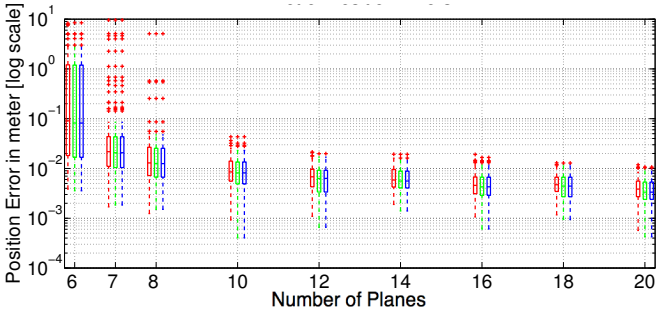

(b) Method 2: Position Error

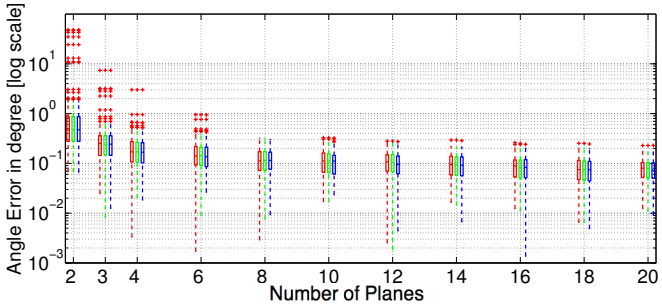

(c) Method 1: Direction Angle Error

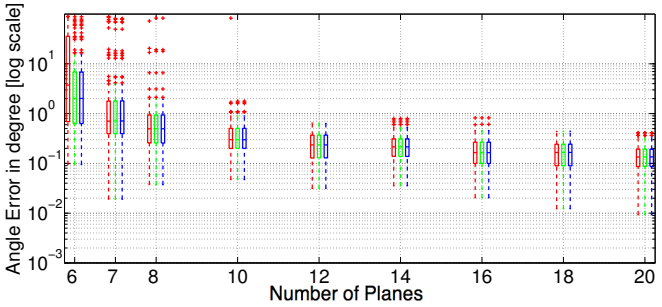

(d) Method 2: Direction Angle Error

Fig. 5: Error distribution for different numbers of measurements for Method 1 (left column) and Method 2 (right column). The pure linear solution is given in red, refined estimate for laser position and direction in green and full optimization including camera intrinsics in blue. The noise level was fixed here to 2D Gaussian noise ($\sigma = 1$ pixel) for the pixel observations, Gaussian noise ($\sigma = 2mm$) for range measurements.

of the laser dot detection varied in a range of approximately 2 pixels or more in few cases.

Similar to evaluation on synthetic data, we also observed that Method 2 needs *well conditioned* plane poses where

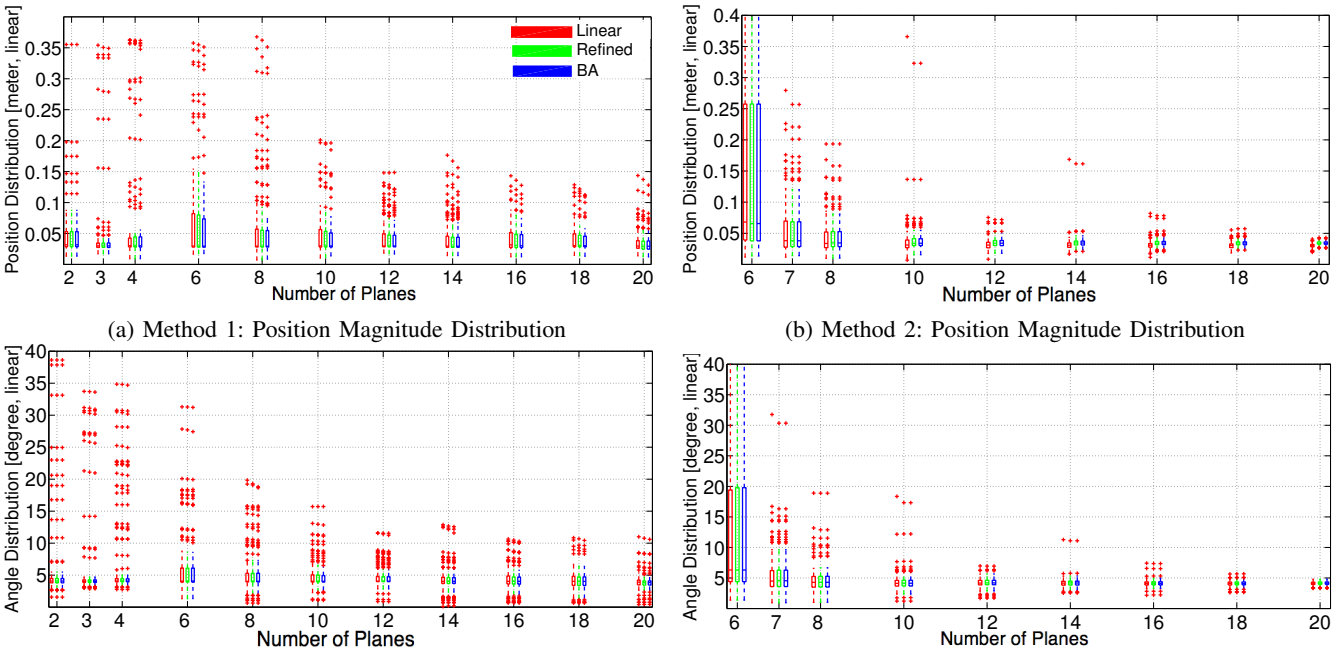

(a) Method 1: Position Magnitude Distribution

(b) Method 2: Position Magnitude Distribution

(c) Method 1: Direction Angle Distribution

(d) Method 2: Direction Angle Distribution

Fig. 6: For both Method 1 (left column) and Method 2 (right column), we plot distribution of the estimated LRF parameters (P,D) for real data including: length of P, and angle between D and camera direction. The pure linear solution is given in red, refined estimate for laser position and direction in green and full optimization including camera intrinsics in blue.

angles between the planes cover a range up to 90 degrees.

IV. Conclusion and Future Work

We proposed two methods for calibrating the relative pose of a single point laser range finder with respect to a camera. Method 1 requires range observations and 2D observation of the laser dot in the corresponding frame; while Method 2 requires only range observations dispensing with any further image processing, or in setups where the laser is not visible in the camera image at all. Both methods can be used with any normal camera calibration method using multiple images of known targets. Furthermore, we described how the methods are integrated with normal camera calibration and how to model a joint optimization of camera and LRF parameters.

Our evaluation on both synthetic data and real data shows that the proposed methods are reliable and accurate, especially Method 1. For the same given number of plane poses, Method 1 performs significantly better than Method 2, according to our evaluation results.

While Method 2 using only laser range observations is clearly more limited compared to the more direct Method 1 using both range observations and detected laser dot, we think that it extends the ranges of possible setups. Therefore, we plan to investigate other possibilities to gain higher accuracy for this type of setups.

References

[1] S. N. Patel, J. Rekimoto, and G. D. Abowd, "iCam: precise at-a-distance interaction in the physical environment," in *Proc. PERVASIVE'06*. Berlin, Heidelberg: Springer-Verlag, 2006, pp. 272–287.

[2] J. Wither, C. Coffin, J. Ventura, and T. Hollerer, "Fast annotation and modeling with a single-point laser range finder," in *Proc. ISMAR '08*. IEEE Computer Society, 2008, pp. 65–68.

[3] Q. Zhang and R. Pless, "Extrinsic calibration of a camera and laser range finder (improves camera calibration)," in *Proc. IROS '04*, vol. 3. IEEE, 2004, pp. 2301–2306.

[4] F. Vasconcelos, J. P. Barreto, and U. Nunes, "A Minimal Solution for the Extrinsic Calibration of a Camera and a Laser-Rangefinder." *IEEE Transactions On Pattern Analysis and Machine Intelligence*, vol. 34, Jan. 2012.

[5] B. Kluge, C. Kohler, and E. Prassler, "Fast and robust tracking of multiple moving objects with a laser range finder," in *Proc. ICRA '01*, vol. 2, 2001, pp. 1683 – 1688.

[6] H. Surmann, A. Nüchter, and J. Hertzberg, "An autonomous mobile robot with a 3d laser range finder for 3d exploration and digitalization of indoor environments," *Robotics and Autonomous Systems*, vol. 45, pp. 181 – 198, 2003.

[7] P. Chakravarty and R. Jarvis, "Panoramic vision and laser range finder fusion for multiple person tracking," in *Proc. IROS '06*, oct. 2006, pp. 2949 –2954.

[8] D. Hahnel, W. Burgard, D. Fox, and S. Thrun, "An efficient fastslam algorithm for generating maps of large-scale cyclic environments from raw laser range measurements," in *Proc. IROS '03*, vol. 1, oct. 2003, pp. 206 – 211 vol.1.

[9] G.-Q. Wei and G. Hirzinger, "Active self-calibration of hand-mounted laser range finders," in *Proc. ICRA 1997*, vol. 4, 1997, pp. 2789–2794.

[10] T. N. Hoang and B. H. Thomas, "In-situ refinement techniques for outdoor geo-referenced models using mobile ar," in *Proc. ISMAR '09*. Washington, DC, USA: IEEE Computer Society, 2009, pp. 193–194.

[11] R. Unnikrishnan and M. Hebert, "Fast extrinsic calibration of a laser rangefinder to a camera," Robotics Institute, Tech. Rep. CMU-RI-TR-05-09, 2005.

[12] A. Vorozcovs, W. Stuerzlinger, A. Hogue, and R. S. Allison, "The hedgehog: A novel optical tracking method for spatially immersive displays," *Presence: Teleoperators and Virtual Environments*, vol. 15, no. 1, pp. 108–121, 2013/03/05 2006.

[13] G. Bradski, "The OpenCV Library," *Dr. Dobb's Journal of Software Tools*, 2000.